Surface Mediated Optical Properties of Ag/NaF Hybrid Crystal Synthesized by Photochemical Process

Min-Jin Ko,*† Waiping Ma, Joel Plawsky, and Heyer Birnboim

†*LG Chemical Ltd., Research Park, Advanced Materials Research Institute, Science Town, Taejon 305-380, Korea*
Department of Chemical and Mechanical Engineering, Rensselaer Polytechnic Institute, Troy, NY12180, USA
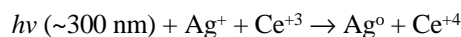*Received August 31, 1998*

Nanometer-sized particles have attracted much attention because of their novel properties as well as large possibility for application. The materials, often referred to as clusters and quantum dots, are intermediate in size between molecular species and a bulk, and show a number of unique behavior such as size quantization[1] and unusual fluorescence.[2] Nanostructured ultrafine metal particles are particularly interesting to study because its dielectric properties are such that it shows a large plasmon resonance. Surface enhanced Raman scattering (SERS) has been found in small particle form.[3] They also hold promise as advanced materials with new electronic, magnetic, optic, and thermal properties.[4]
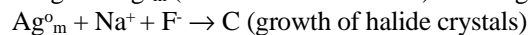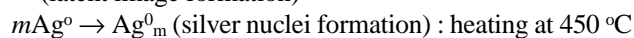
Recently engineered dielectric properties of hetero-structured composite materials have been investigated. Kortan[5] reported that electronic structure of inorganic particles can be changed by layering them with different inorganic substrate. Honma[6] showed the surface enhanced Raman scattering of inorganic particles from metal-inorganic hybrid composite structure. Metal layered hybrid particles have also been suggested as a scheme to provide substantial enhancement of the optical non-linearity.[7] In this communication we report our initial work on the preparation of layered hybrid nanoparticles in a glass matrix by a photochemical process and experimental observation of the red-shift of Ag surface plasmon resonance and the resonance dependence of the nonlinear optical behavior.

For the synthesis of Ag laden sodium halide nanocrystallites, the photochemical process, including two UV exposures and two heat-treatments, is used. All constituents of glasses were batched with use of reagent grade materials and melted in covered platinum crucibles. Batch materials included high purity sodium carbonate, calcined alumina, zinc oxide, antimony trioxide and sodium silicofluoride (F⁻, 2-5%). On the melting and subsequent cooling, they became supersaturated solutions of NaF. They also contained the sensitizers Ag^+ and Ce^{+3} (0.01-0.1%). The glasses were melted at 1400-1500 for 4-5 h, and stirred before being poured into slabs and annealed at 400 °C overnight to release internal stresses and then cooled slowly. The stress free glasses were cut into thin slices and the surface was polished on SiC paper followed by final polishing using a cerium oxide slurry. The glass is first subject to an UV exposure in order to cause Ce^{+3} to eject an electron which is captured by Ag^+, for 10 sec to 5 min, and subsequently heated to about 450 °C for 15 min and 520 °C for 1 h. The first heat treatment causes the silver metal to agglomerate and then nucle-
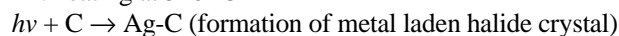
ate the growth of the sodium halide crystals controlled by the duration of the heat-treatment. The second exposure and heat treatment further reduce the remaining silver which then diffuses to, and coats the outside of the NaF crystals. Typical UV exposure time was about 10 min ~1 h and heat-treatment was conducted at 425 °C. The reduction and growth mechanism of Ag^+ follow as

hv (~300 nm) + Ag^o + Ce^{+3} → Ag^o + Ce^{+4}
    (latent image formation)
mAg^o → $Ag^0{}_m$ (silver nuclei formation) : heating at 450 °C
$Ag^o{}_m$ + Na^+ + F^- → C (growth of halide crystals)
    : heating at 520 °C
hv + C → Ag-C (formation of metal laden halide crystal)
    : heating at 425 °C
where C = NaF crystal and Ag-C = Ag laden NaF crystal.

The thickness of silver is controlled by the fluence of the UV exposure. Ultraviolet exposures were made using HgXe arcs, typically high-pressure lamps operating at about 2000 W with collimation. Glass filters were used to control the fluence of the UV exposure. The essential requirement was a substantial flux of ultraviolet light in the 280-320 nm band at which the Ce^{+3} is activated.

A series of absorption spectra for the glass substrate after the UV exposures and heat-treatments are shown in Figure 1. The first UV exposure was ranging from 10 sec to 2 min with a 15 or 20 sec interval and second UV exposure was
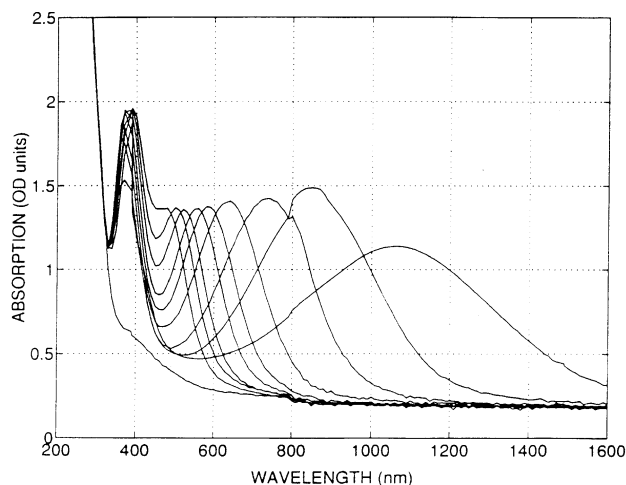

Figure 1. Absorption spectra of the glass substrate after heat-treatments and UV exposures.

Communications to the Editor

Bull. Korean Chem. Soc. **1999**, Vol. 20, No. 1   25

conducted up to 30 min to control maximum optical density. The absorption band appeared over the visible wavelength range results in the full color of the transparent sample. Unlike the isolated spherical Ag particles, it is shown that on each absorption spectrum curve a distinct pair of plasmon resonances are observed. The wavelengths of the pair can be tuned from 420 nm to 370 nm for the high energy plasmon resonance and from 420 nm to 1100 nm for the low energy plasmon resonances. The location of the secondary absorption band was a sensitive function of the amount of UV exposure. The low level of first UV exposure (UV exposure for 10 sec) gave a secondary absorption band at 1100 nm wavelength while the high level of first UV exposure (UV exposure for 2 min) at 480 nm. We think that two plasmon resonances in this experiment is due to the Ag/NaF hybrid particles, not to the isolated Ag particles. Only one Ag plasmon peak at about 400 nm peak was appeared without NaF phase. It is also hard to believe that isolated elongated Ag particles is formed without any external stress. Elongated Ag particles in glass can be formed by stretching the melt during cooling process. Thus the red-shifted plasmon resonances in Figure 1 is clearly indicative of a layered Ag metal particles on NaF crystals.

In order to understand the broad absorption peak in Figure 1 shifted to longer wavelength compared to that of a dispersion of homogeneous Ag particles, the optical absorption of layered spherical particles has been calculated based on the Birnboim *et al.* model.[7] The particle consists of a core of radius $r1$ covered with a uniform spherical shell, giving a total particle radius $r2$. The dielectric constitutive equation for the inhomogeneous composite of core, shell and host medium can be represented as an equivalent homogeneous medium of dielectric permittivity, $\tilde{\varepsilon}$. Since, in our case, the volume fraction of the particles is very small, interparticle effects can be neglected. This leads to an expression of the Maxwell-Garnett form, which to the first order in particle volume fraction ρ, is

$$\tilde{\varepsilon} = \varepsilon_3 + 3\rho\varepsilon_3 \frac{\varepsilon_2\varepsilon_a - \varepsilon_3\varepsilon_b}{\varepsilon_2\varepsilon_a + 2\varepsilon_3\varepsilon_b}, \qquad (1)$$

where $\varepsilon_a = \varepsilon_1[3-2P]+2\varepsilon_2 P, \varepsilon_b = \varepsilon_1 P + \varepsilon_2[3-P], P = 1-(r1/r2)^3$. ε_1 is the dielectric constant of core material, ε_2, the dielectric constant of shell material, ε_3, the dielectric constant of

the glass host, and P the ratio of shell volume to total particle volume. Total extinction of the composite will have a loss contribution from intrinsic molecular absorption and a loss contribution from particle scattering. Optical absorption characteristics of this model were calculated in the Rayleigh approximation since the dimensions of the particles of our samples are much smaller than the wavelengths of the visible light, and, thus, scattering loss is negligible. The extinction coefficient, α, is given by

$$\alpha = (2\pi / \lambda_0 \tilde{n}')\tilde{\varepsilon}'' / \varepsilon_0, \qquad (2)$$

where λ_0 is the vacuo wavelength, $\tilde{n}$ is effective refractive index at the vacuo wavelength and is $(\varepsilon_3 / \varepsilon_0)^{1/2}$, and ε'' is the imaginary part of the effective dielectric constant and is obtained from equation (1). We assume that metal shell volume fraction parameter, P, is proportional to the UV exposure. The low energy plasmon resonance peaks fit the model well. On the other hand, the high energy resonance peaks range from 370 to 390 nm. Table 1 shows the comparison of experimental data and model calculation for both the positions of the pair of resonances λ_1 and λ_2 and their line widths $\triangle\lambda_1$ and $\triangle\lambda_2$. The some discrepancy between calculated and observed line widths are attributed to a non-uniform distribution of shell thickness. The line widths $\triangle\lambda_2$ for the low energy peaks
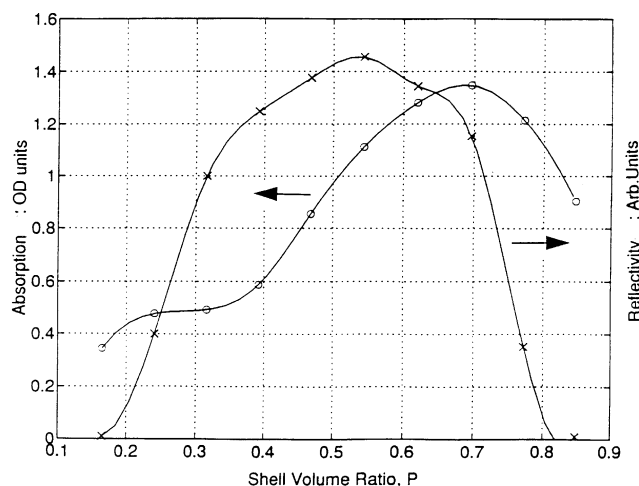

Figure 2. Conjugate reflection of glass samples and absorption spectra measured at 532 nm as shell volume ratio.

Table 1. Comparison of measured and calculated high and low energy absorption peak position and line width. In the calculation, the shell volume ratio P is adjusted so that the low-energy absorption peak positions match the experimental results

Volume ratio(P)	0.18	0.28	0.37	0.48	0.58	0.62	0.7	0.75	0.8	1
λ1(expt.)	370	360	360	370	370	380	380	390	390	-
λ1(theory)	325	325	330	330	330	330	330	330	330	420
$\triangle$ λ1(expt.)	115	105	100	100	105	115	130	120	120	-
$\triangle$ λ1(theory)	10	11	13	8	8	8	10	10	10	9
λ2(exp.)	1060	850	740	640	580	560	520	500	480	-
λ2(theory)	1060	850	740	640	580	560	520	500	480	420
$\triangle$ λ2(expt.)	700	405	315	250	220	180	150	135	110	-
$\triangle$ λ2(theory)	19	18	18	16	15	15	14	13	12	-

are most sensitive to shell thickness variation Nonlinear optical measurements by degenerate four wave mixing (DFWM) have been conducted on the metal laden sodium halide samples. The primary laser source consisted of a Q-switched and mode-locked Nd:YAG laser, a pulse switch, and an amplifier. Counter propagating pump beams of equal intensity strike on sample from opposite directions. A probe beam is incident at an angle of ~5° with respect to the forward pump. The conjugate signal is separated from the probe beam with a beam splitter and is measured with a photomultiplier. A liquid crystal pulse modulated polarization rotator placed into the probe beam path to distinguish between conjugate signal and noise from sample surface scattering. The results are shown in Figure 2 which plots the relative intensity of the conjugate signals at 532 nm from the series of the samples, together with the measured absorption (in OD units) of each sample at 532 nm. This figure clearly demonstrates the plasmon resonance enhancement of intrinsic nonlinearity. No discernible peak was observed in the isolated Ag particles or NaF particles in glass. It was found to be about several orders of magnitude larger than nonlinear susceptibility of the isolated NaF and Ag particles at this wavelength. The results of the study of the nonlinear optical properties of these composite materials will be discussed in detail in a future publication.

In summary, we have synthesized and characterized metal particles laden inorganic crystal in glass by photochemical process with optical properties. The layered Ag nanoparticles show the two plasmon resonances and this phenomenon is described with a model based on the effective medium theory. NLO measurements on this composites show the strong plasmon resonance enhancement of intrinsic nonlinearity. Further experiments are being designed to elucidate the structural effects of the hybrid composites on linear and nonlinear optical properties and to synthesize the hybridized particles containing various inorganic particles.

References

1. (a) Brus, L. E. *J. Chem. Phys.* **1984**, *80*, 4403. (b) Hasselbarth, A.; Eychmuller, A.; Weller, H. *Chem. Phys. Lett.* **1993**, *203*, 271. (c) Ekimov, A. I.; Onushchenko, A. A. *Sov. Phys. Semicond.* **1982**, *16*, 775. (d) Borrelli, N. F.; Hall, D. W.; Holland, H. J.; Smith, D. W. *J. Appl. Phys.* **1987**, *61*, 5399.

2. (a) Misawa, K.; Yao, H.; Hayashi, T.; Kobayashi, T. *Chem. Phys. Lett.* **1991**, *183*, 113. (b) Hache, F.; Klein, M. C.; Ricard, D.; Flytzanis, F. *J. Opt. Soc. Am. B* **1991**, *8*, 1802. (c) Lee, K. C. *Surface Science* **1985**, *163*, 759.

3. (a) Chen, M. C.; Tsai, S. D.; Chen, M. R.; Ou, S. Y.; Li, W. H.; Lee, K. C. *Phys. Rev. B* **1995**, *51*, 4507. (b) Alivisatos, A. P. *Science* **1996**, *271*, 932. (c) Freeman, R. G.; Grabar, K. C.; Allison, K. J.; Bright, R. M.; Davis, J. A.; Guthrie, A. P.; Hommer, M. B.; Jackson, M. A.; Smith, P. C.; Walter, D. G.; Natan, M. J. *Science* **1995**, *267*, 1629.

4. Schmid, G. *Clusters and Colloids*; VCH: Weinheim, **1994**.

5. Kortan, A. R.; Hull, R.; Opila, R. L.; Bawendi, M. G.; Steigerwald, M. L.; Carroll, P. J.; Brus, L. E. *J. Am. Chem. Soc.* **1990**, *112*, 1327.

6. Honma, I.; Sano, T.; Komiyama, H. *J. Phys. Chem.* **1993**, *97*, 6692

7. (a) Neeves, A. E.; Birnboim, M. H. *J. Opt. Soc. Am.* **1989**, *B6*, 787. (b) Haus, J. W.; Kalyaniwalla, N.; Inguava, R.; Bowden, C. M. *J. Appl. Phys.* **1989**, *65*. 1420. (c) Kalyaniwalla, N.; Haus, J. W.; Ingura, R.; Birnboim, M. H. *Phys. Rev. A* **1990**, *42*, 5613.